



Comparison of the structure, electronic, and optical behaviors of tin-doped CdO alloys and thin films

M. S. Othman¹ · Kh. A. Mishjil² · H. G. Rashid² · S. S. Chiad² · N. F. Habubi² · I. A. Al-Baidhany²

Received: 28 December 2019 / Accepted: 17 April 2020 / Published online: 23 April 2020
© Springer Science+Business Media, LLC, part of Springer Nature 2020

Abstract

Spray pyrolysis technique (SPT) was applied to fabricate CdO films doped with tin at (0–8%) concentrations on glass substrates. Structural, morphological, and optical behaviors were inspected using X-ray diffraction (XRD), scanning electron microscopy (SEM), and UV–Vis spectroscopy. Structural, electronic, and optical behaviors of Cd_{1-x}OSn_x alloys were studied in pseudo-potential method using density functional theory (DFT) in scissors approximation. The calculated electronic band structure and optical behavior were achieved in this work. Optical bandgap energy was found to increase from 2.581 to 2.943 eV via increasing Sn content, while theoretically, it was found to increase from 2.884 to 3.106 eV with the increasing Sn doping. Theoretical and experimental findings were close to each other. The linear energy-dependent dielectric functions (real part) and optical behavior-like absorbance and transmittance were also studied.

1 Introduction

One of the important oxide semiconductors is cadmium oxide (CdO). It was used in some applications including solar cells, smart windows, optical communications, anti-reflection coatings, and flat panel display photodiodes [1–3], depending on their electrical and optical behaviors. Pure CdO doped with Sn exhibit semiconducting behavior with good electrical conductivity; in addition, it has transparency in the visible region with direct bandgap energy of 2.54–3.10 eV which increased with doping Sn element [4, 5]. The control of CdO conductivity is difficult during the process of film preparation. CdO can be tuned by doping a number of materials such as S, Pb, Al, In, and Ti [5, 6]. It was realized that doping of Pb, Al, Ti promotes energy bandgap, leading to an increase in electrical conductivity [7–9].

The present study emphasized on CdO compound by doping thin-film Sn element and alloys due to their significance in contemporary electronic devices. This study implied that while Sn concentrations were doped to the compound, optical energy bandgap increased theoretically

and experimentally. This plays a great role in optoelectronic devices and optical behaviors in those alloys and thin film. Investigation of some optical properties in those alloys has been performed.

In the present work, pure CdO was considered experimentally. 2–8% of Sn was doping agent for CdO films. Structural and optical properties are measured. While structural, electronically and optical performance of Cd_{1-x}OSn_x alloys for x composition at a constant temperature have been pointed out once more and they were obtained as well, in which (DFT) was used [10].

2 Methods

2.1 Experimental procedure

Thin films of CdO and Sn-doped CdO were obtained using SPT. An aqueous solution of 0.1 M CdCl₂ was dissolved in deionized water to prepare cadmium oxide. 0.1 M of SnCl₄·5H₂O was used as a doping agent at a concentration of 2–8%. This solution was deposited onto a preheated glass substrate kept at 400 °C. After many trials, the parameters reached the optimal values: Substrate-to-nozzle distance, 30 cm; spraying rate, 5 mL/min; spraying time, 10 s followed by 1 min wait to stop extravagant cooling; and nitrogen as carrier gas. Gravimetric method was used to evaluate thickness, and their values were found to be in the range of

✉ N. F. Habubi
nadirfadhil@uomustansiriyah.edu.iq

¹ Genereal Science Department, Faculty of Education, Soran University, Erbil, Kurdistan Region, Iraq

² Department of Physics, College of Education, Mustansiriyah University, Baghdad, Iraq

350 ± 50 nm. Transmittance and absorbance were obtained via a double-beam spectrophotometer (Shimadzu UV-1650). XRD was used to analyze the film structure. SEM was used to estimate the film morphology. Topography was determined by AFM (AA3000 SPM).

2.2 Theoretical model

Physical behaviors of Cd_{1-x}OSn_x alloys were investigated using the CASTEP program [11]. Calculation in this program is implemented via Kohn–Sham formation, based on DFT. Generalized Gradient Approximation (GGA) is made for electronic exchange–correlation potential energy, which was brought about by electron–ion interaction [12]. A cubic unit cell is constructed with (Cd/Sn).

One of the models used in Cd_{1-x}OSn_x ternary alloys was wurtzite. A 16-atom super cell was applied that matches 2 × 2 × 1 and is twice of wurtzite unit cell, concerning the size in the initial plan. Pseudo-potential concept was used to describe Coulomb potential energy, which was led by electron–ion interaction.

The scheme suggested by Liou et al. [13] was used to adopt the optimized non-local pseudo-potential, in which orbitals including Cd (4d¹⁰ 5s²), O (2s² 2p⁴), and Sn (4d¹⁰ 5s² 5p²) played role as valence electrons.

A kinetic energy cutoff of 890 eV was used in plane waves, as the wave function was prolonged. Furthermore, the k-point of 5 × 5 × 4 was applied for x = 0.5 and 6 × 6 × 6 for the other composition x. In the present work, the proportion between the Cd, O, and Sn atoms was identified for every alloy.

The specified electronic energy bandgaps (E_g) are at the Γ point for crystalline alloys in the bulk structure using electronic exchange–correlation energy.

Cd_{1-x}OSn_x alloys with cubic symmetry in the calculations were indicated for the five systems to continue regularity and easiness. The expectation was that for x = 0, 0.25, 0.5 and 0.75, non-cubic structure for the layered alloy. The first step of Geometry Optimization was achieved for Cd_{1-x}OSn_x alloys for x compositions with symmetry P1. Figure 1 shows the optimization step only for x = 0.75 as an example.

Equilibrium lattice constant was calculated from high symmetry directions in first Brillouin zone and corresponding density of the states. Calculations of band structures well matched with each other for CdOSn alloys.

The optical behaviors were indicated for all alloys. The dielectric equation $\epsilon(\omega) = \epsilon_1(\omega) + i\epsilon_2(\omega)$ was utilized for describing linear response, resulting from interaction of photons with electrons [14]. The real part $\epsilon_1(\omega)$ of dielectric equations was calculated using Kramers–Kronig relation [15]. Complex dielectric function embraced other optical behaviors. Below are some of the terms used to express dielectric functions [16, 17]:

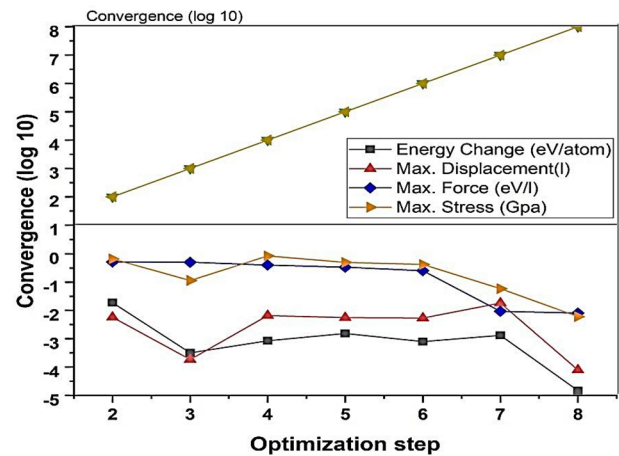


Fig. 1 Optimization step convergence of Cd_{1-x}OSn_x for x = 0.75

$$\epsilon_1(\omega) = 1 + \frac{2}{\pi} \int_0^{\infty} \frac{\epsilon_2(\omega') \omega' d\omega'}{\omega'^2 - \omega^2}; \quad (1)$$

$$\epsilon_2(\omega) = \frac{Ve^2}{2\pi\hbar m^2 \omega^2} \int d^3k \sum_{nn'} \left| \langle kn | p | kn' \rangle \right|^2 f(kn) \times [1 - f(kn')] \delta(E_{kn} - E_{kn'} - \hbar\omega), \quad (2)$$

where $\hbar\omega$ is incident photon energy, p is the momentum $\frac{\hbar}{i} \frac{\partial}{\partial x}$, $|kn\rangle$ is the eigenfunction with eigenvalue E_{kn} , and $f(kn)$ is Fermi distribution function;

$$\alpha(\omega) = \sqrt{2\omega} \left[\sqrt{\epsilon_1^2(\omega) + \epsilon_2^2(\omega)} - \epsilon_1(\omega) \right]^{1/2}. \quad (3)$$

Using these relations of Eqs. (1)–(3), real part of the dielectric functions $\epsilon_1(\omega)$ and absorption $\alpha(\omega)$ were calculated.

3 Results and discussion

Figure 2 displays XRD patterns of the prepared CdO doped with 0% (undoped), 2%, 4%, 6%, and 8% Sn, respectively. All the films display mainly CdO diffraction peak at (111), (200), (220) planes assigned to ICDD card no. 005-0640. Diffraction peaks of Sn at (211) and (200) corresponds to ICDD card no. 04-0673. These peaks confirm the formation of polycrystalline CdO, which agreed with the results gained by Kathalingam et al. and Makori et al. [18, 19]. To obtain the detailed structure information, the crystallite size (D) was evaluated using Debye–Scherrer's equation [20]:

$$D = \frac{0.94}{B \cos \theta}, \quad (4)$$

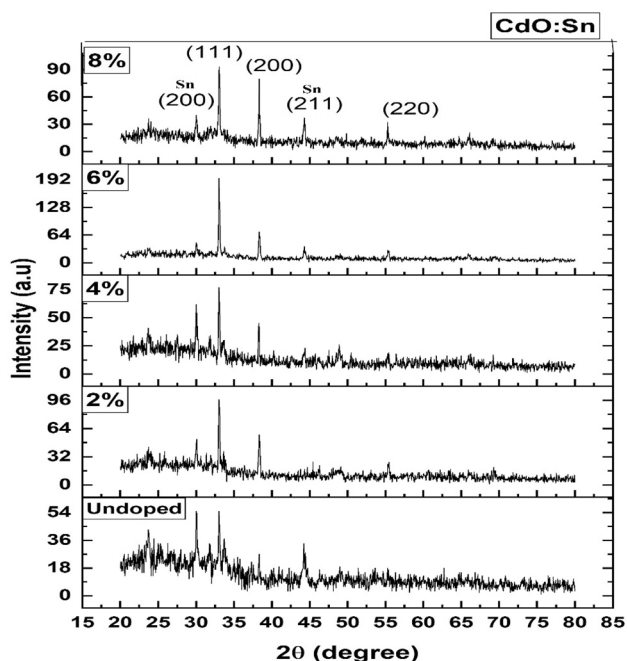


Fig. 2 XRD patterns of CdO doped with (0–8%) Sn, respectively

where B , λ , θ is the FWHM, X-ray wavelength, Bragg's angle, respectively. D increases with increasing Sn content; hence the order of crystallinity was improved by doping.

Figure 3a–e depicts SEM images of CdO doped with (0–8%) Sn. The CdO doped with 8% Sn content has the best regular surface, referring that Sn doping affects the crystalline structure and changes the film morphology as displayed by SEM images.

The thin films have regular surface morphologies with spherical combinations composed of nanoparticles. By increasing Sn content, surface morphology of CdO films changed significantly. When Sn concentration increases, the crystallite size also progressively increases. These results were confirmed by the XRD results and agrees with the reported results of León-Gutiérrez et al. [21].

The minimizing lattice parameter of the crystal was used to calculate lattice constants of alloys at equilibrium. The lattice parameters discovered were 4.612, 4.781, 4.790, and 4.808 Å for $\text{Cd}_{1-x}\text{OSn}_x$ alloys for $x = 0, 0.25, 0.5, \text{ and } 0.75$, respectively. In the Γ direction, the calculated alloys got direct bandgap energy. Table 1 indicates the results of the present work.

Table 1 displays the bandgap energies (E_g) based on Sn concentration. As E_g increases from 2.581 to 2.943 eV, x composition of alloys increases. The bandgap energy in theoretical data is less than the experimental data due to the usage of the GGA calculation.

Table 1 also displays the achieved findings including theoretical and experimental data of energy bandgap values. The results were in consistent with other studies [19, 22].

In Fig. 4, the experimental results of $(\alpha h\nu)^2$ against $h\nu$ of the deposited thin films are presented. The bandgap energies increased as the value of Sn content increased.

Figure 5 represents the increase of the optical bandgap energies in experimental and theoretical data with an increase in Sn content. It was approximately an increase about zero in bandgap energies value with increase in Sn concentration and it referred to a proof of decreased conduction band edge with an increase in doping concentration [22]. Figure 6 includes (a) theoretical and (b) experimental dielectric function data of the real part.

Figure 6a and b also indicates that as the energy increases, the dielectric function increases too likewise out of the region between 1.98 and 3.85 eV. All these are called normal dispersion. Though strong absorption and increase in reflection were presented at 2.13–3.48 eV, it was clarified in the absorption data.

These alloys have limitation of essential absorption at visible and near-infrared spectrum regions. These regions are effective for electronic devices. Figure 6a and b shows the calculation of static dielectric constant $\epsilon_1(0)$ and their values are listed in Table 1.

Figure 7 provides information about optical absorption spectra of $\text{Cd}_{1-x}\text{OSn}_x$ alloys under scissor operation. Due to underestimation of energy bandgap, it is hard to gain the exact optical energy bandgap. In theoretical calculations, energy scissor approximation with 0.6 eV to fit the absorption edge was utilized in the experimental value as seen in Fig. 5a and b. This process can be considered as a successful way for various systems [23]. Tauc's equation interpreted the relation between E_g and the absorption coefficient (α) [24]:

$$\alpha h\nu = c(h\nu - E_g), \quad (5)$$

where c is a constant. E_g was achieved by plotting $(\alpha h\nu)^2$ via $h\nu$. E_g of alloys was also gained using extrapolation.

In Fig. 8, the optical absorbance of the deposited films were displayed. For wavelengths less than 450 nm, the absorbance became very high for doped films. The doping demonstrates an enhancement in film structure and increase in the grain size, which agrees with Chowdhury et al. [25].

In Fig. 9, the experimental transmittance spectra of CdO and Sn-doped CdO can be seen. The results of experimental data have indicated that the transmittance was found to be 88% for the undoped film, while transmittance declines with Sn contents as 78%, 77%, 71%, and 69% for 2%, 4%, 6%, and 8%, respectively, in visible and near-infrared region (450–850 nm). The increased photon scattering by crystal defects/doping leads to a

Fig. 3 a–e SEM images of CdO doped with (0–8%) Sn

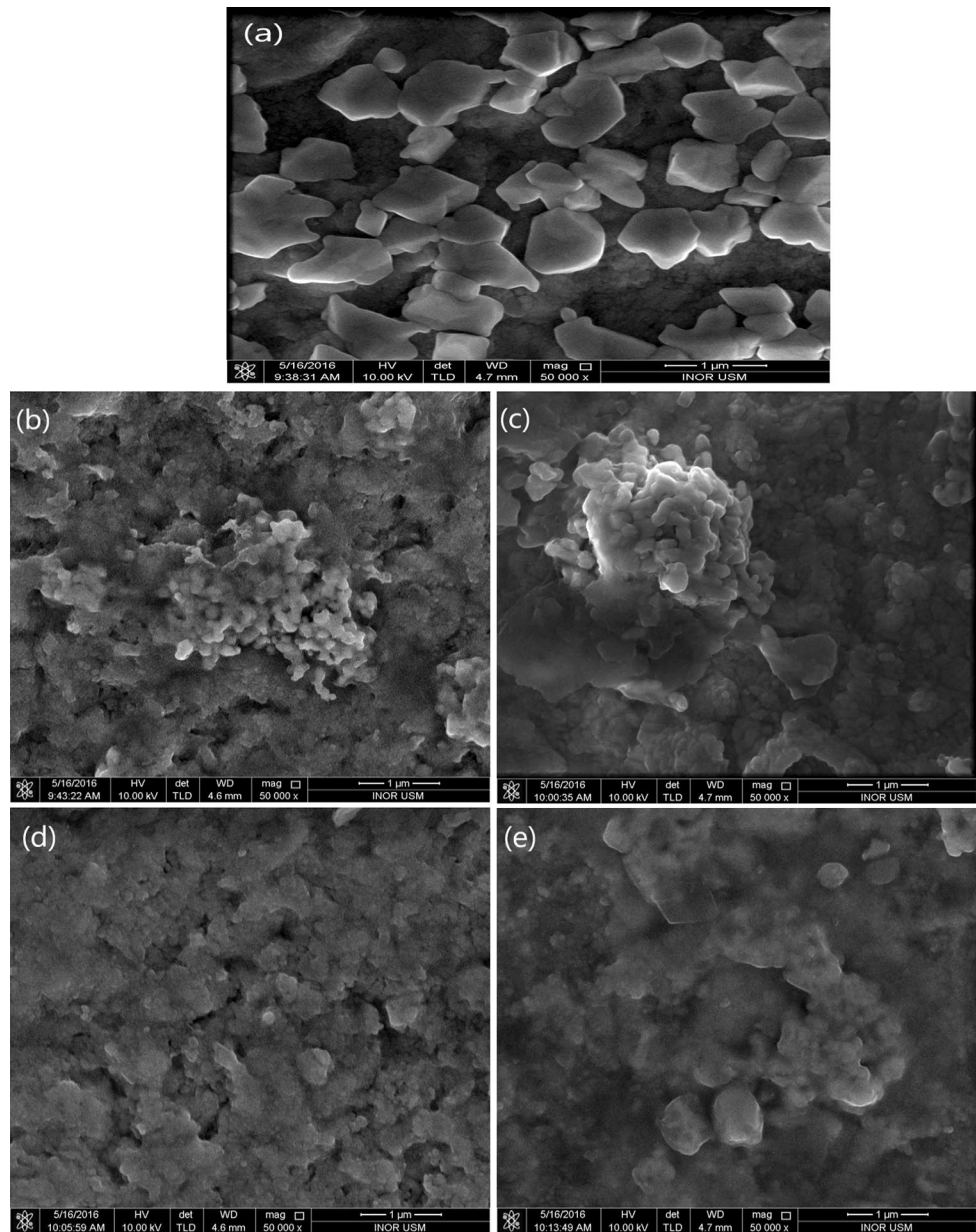


Table 1 Average transmitters (AT), optical energy bandgap (E_g), and optical dielectric constant $\epsilon(0)$ of the deposited films

Sn (%) present	AT (%) (exp.)	(E_g) eV (exp.)	$\epsilon(0)$	Materials (present)	AT (%) (theory)	(E_g) eV (theory)	$\epsilon(0)$
0	88.901	2.884	2.635	0	87.21	2.581	13.986
2	78.937	2.953	3.797	0.25	77.63	2.619	11.614
4	77.983	2.979	3.865	0.50	72.41	2.791	13.083
6	71.640	3.004	4.606	0.75	69.34	2.943	12.591
8	69.815	3.106	4.790	–	–	–	–

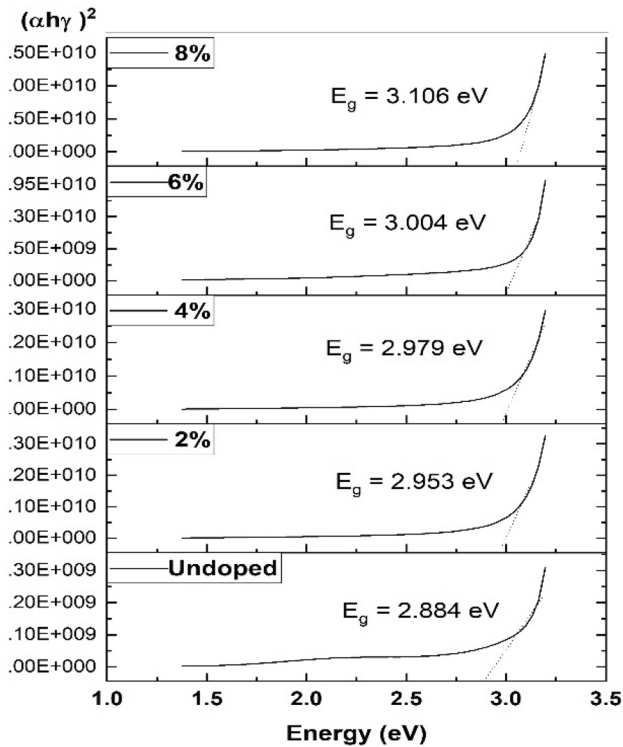


Fig. 4 Experimental variation of $(\alpha h\nu)^2$ versus $(h\nu)$ of Sn-doped CdO films

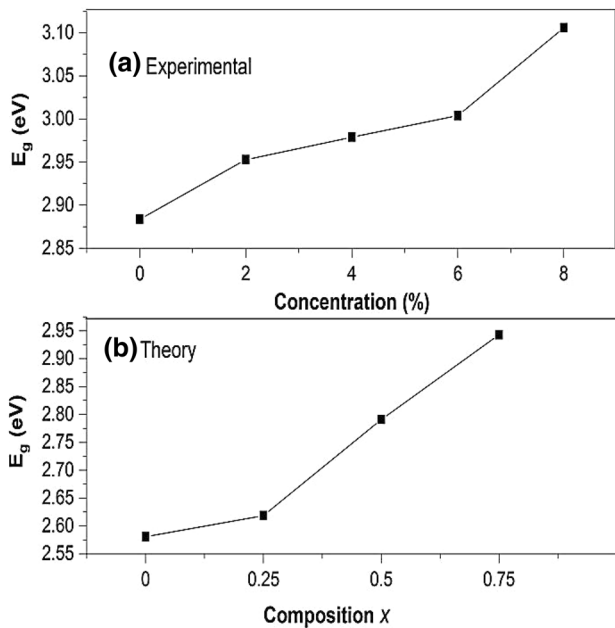


Fig. 5 a, b Increase in the determined optical bandgap energies theoretically and experimentally via increasing Sn content

decrease in transmittance [24]. The optical transmittance is effectively linked to its surface morphology.

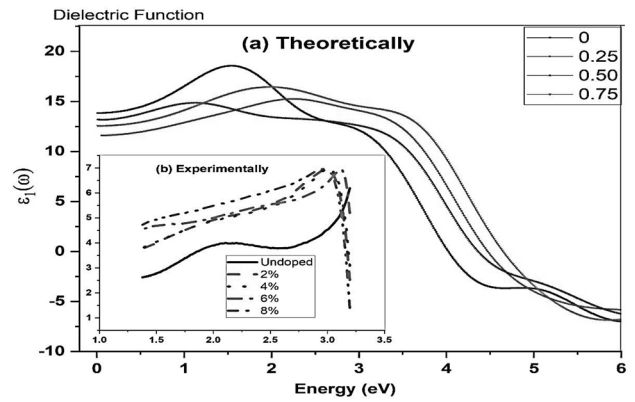


Fig. 6 (a, b) Real part of dielectric function

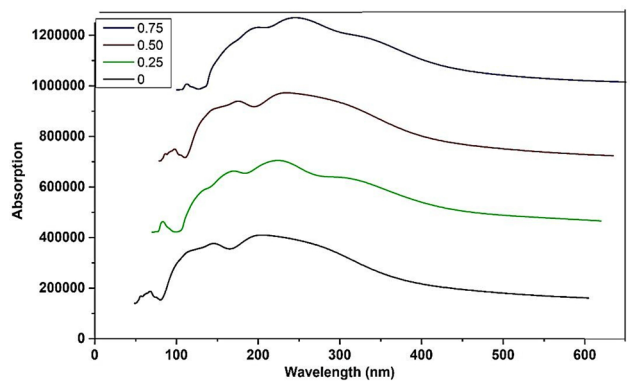


Fig. 7 Optical absorption (theoretical) of the $Cd_{1-x}Sn_x$ alloys

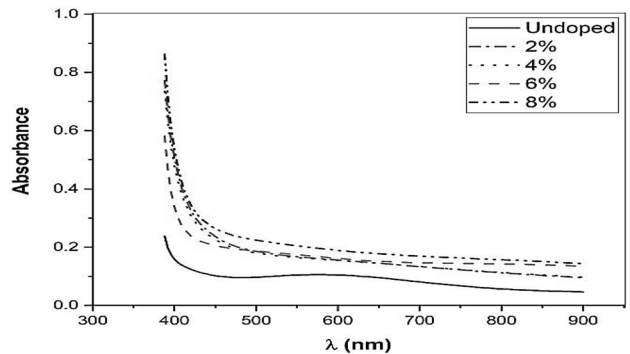


Fig. 8 Absorbance (experimental) of the deposited films

The transmittance spectra (theoretical) of CdO and Sn-doped CdO are shown in Fig. 10. Transmittance declines with x compositions as 87%, 75%, 72%, and 67% for 0, 0.25, 0.50, and 0.75, respectively, in visible and near-infrared region (460–840 nm). In addition, for the theoretical results, it found that the transmission decreases with increasing Sn. According to the findings, the values of theoretical and

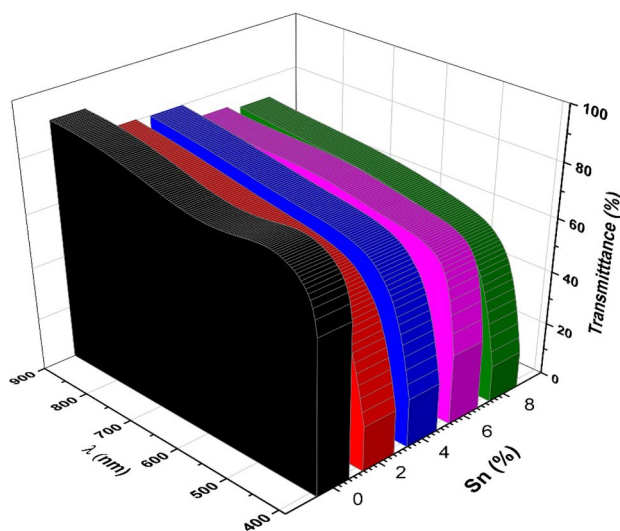


Fig. 9 Transmittance (experimental) of the deposited films

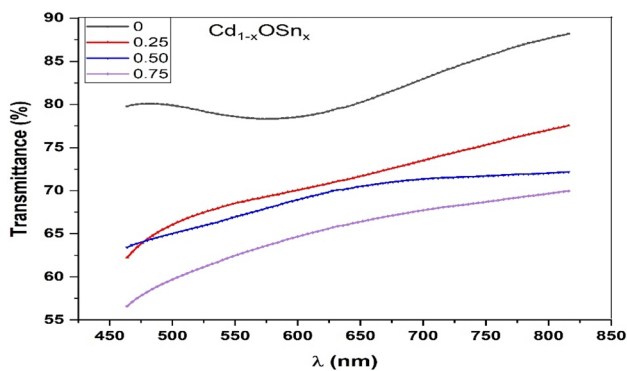


Fig. 10 Transmittance (theoretical) of the deposited alloys

experimental data agreed with each other, and it is consistent with Ronconi and Kumaravel's results [26, 27].

4 Conclusions

To sum up the theoretical results, electronic and optical properties of the $\text{Cd}_{1-x}\text{OSn}_x$ alloys using the DFT calculations based on the plane-wave pseudo-potentials method within the GGA approximation were pointed out. The calculations were performed for the lattice constants (4.612, 4.781, 4.790, and 4.808 Å for $\text{Cd}_{1-x}\text{OSn}_x$ alloys for $x = 0, 0.25, 0.5, \text{ and } 0.75$), energy bandgap, and optical properties.

In the electronic structures, energy gap also increased from 2.581 to 2.941 eV in theoretical findings with increasing tin doping concentration for x compositions. These results are in agreement with experimental data increased

from 2.884 to 3.106 eV. All data were closely compatible in electronic properties with doped thin films.

Experimental and theoretical findings consider that the transmittance decreases with doping from 78%, 76%, 65%, and 61% for 2%, 4%, 6%, and 8% Sn-doped CdO, respectively. Also in theory section Transmittance declines with x compositions as 87%, 75%, 72% and 67% for 0, 0.25, 0.50, and 0.75, respectively, in visible and near-infrared regions.

Electronic and optical behaviors of these alloys and thin films with Sn concentration (theoretical and experimental) can be taken into consideration for electronic devices and applications. It can also be used as an effective and beneficial reference for technological life.

Acknowledgements The authors appreciate Mustansiriyah university for their support.

References

1. R. Chandiramouli, B.G. Jeyaprakash, Review of CdO thin films. *Solid State Sci.* **16**, 102–110 (2013)
2. F. Yakuphanoglu, Synthesis and electro-optic properties of nano-sized-boron doped cadmium oxide thin films for solar cell applications. *Sol. Energy* **85**(11), 2704–2709 (2011)
3. M. Othman, S. Salih, M. Sedighi, E. Kasap, Impact of pressure and composition on the mechanical behavior of $\text{In}_x\text{Ga}_{1-x}\text{As}_{1-y}\text{Py}$ and $\text{Al}_x\text{In}_{1-x}\text{Sb}_{1-y}\text{Py}$ quaternary alloys. *Results Phys.* **14**, 102400 (2019)
4. M. Thambidurai, N. Muthukumarasamy, A. Ranjitha, D. Velauthapillai, Structural and optical properties of Ga-doped CdO nanocrystalline thin films. *Superlattices Microstruct.* **86**, 559–563 (2015)
5. Z. Zhao, D.L. Morel, C.S. Ferekides, Electrical and optical properties of tin-doped CdO films deposited by atmospheric metalorganic chemical vapor deposition. *Thin Solid Films* **413**(1–2), 203–211 (2002)
6. B. Saha, R. Thapa, K.K. Chattopadhyay, Bandgap widening in highly conducting CdO thin film by Ti incorporation through radio frequency magnetron sputtering technique. *Solid State Commun.* **145**(1–2), 33–37 (2008)
7. B.J. Zheng, J.S. Lian, L. Zhao, Q. Jiang, Optical and electrical properties of In-doped CdO thin films fabricated by pulse laser deposition. *Appl. Surf. Sci.* **256**(9), 2910–2914 (2010)
8. R.K. Gupta, K. Ghosh, R. Patel, S.R. Mishra, P.K. Kahol, Influence of oxygen partial pressure on optoelectrical properties of aluminum-doped CdO thin films. *Appl. Surf. Sci.* **254**(18), 5868–5873 (2008)
9. A.A. Dakhel, Structural, optical and electrical measurements on boron-doped CdO thin films. *J. Mater. Sci.* **46**(21), 6925–6931 (2011)
10. M. Othman, E. Kasap, N. Korozlu, Ab-initio investigation of structural, electronic and optical properties of $\text{In}_x\text{Ga}_{1-x}\text{As}$, $\text{GaAs}_{1-y}\text{Py}$ ternary and $\text{In}_x\text{Ga}_{1-x}\text{As}_{1-y}\text{Py}$ quaternary semiconductor alloys. *J. Alloy. Compd.* **496**(1–2), 226–233 (2010)
11. M. Othman, E. Kasap, N. Korozlu, The structural, electronic and optical properties of $\text{In}_x\text{Ga}_{1-x}\text{P}$ alloys. *Phys. B* **405**(10), 2357–2361 (2010)
12. M.S. Othman, Simulation mechanical properties of lead sulfur selenium under pressure. *J. Mod. Phys.* **4**(02), 185 (2013)

13. B.T. Liou, C.Y. Lin, S.H. Yen, Y.K. Kuo, First-principles calculation for bowing parameter of wurtzite $\text{In}_x\text{Ga}_{1-x}\text{N}$. *Opt. Commun.* **249**(1–3), 217–223 (2005)
14. H. Akkus, A.M. Mamedov, Ab initio calculations of the electronic structure and linear optical properties, including self-energy effects, for paraelectric SbSI . *J. Phys.* **19**(11), 116207 (2007)
15. M. Othman, E. Kasap, N. Korozlu, Ab-initio investigation of electronic and optical properties of $\text{InAs}_{1-x}\text{Px}$ alloys. *Gazi Univ. J. Sci.* **23**(2), 149–153 (2009)
16. H. Dammak, A. Yangui, S. Triki, Y. Abid, H. Feki, Structural characterization, vibrational, optical properties and DFT investigation of a new luminescent organic–inorganic material: $(\text{C}_6\text{H}_{14}\text{N})_3\text{Bi}_2\text{I}_9$. *J. Lumin.* **161**, 214–220 (2015)
17. M.S. Othman, K.A. Mishjil, N.F. Habubi, Structural and optical properties of $\text{GaAs}_{0.5}\text{Sb}_{0.5}$ and $\text{In}_{0.5}\text{Ga}_{0.5}\text{As}_{0.5}\text{Sb}_{0.5}$: ab initio calculations for pure and doped materials. *Chin. Phys. Lett.* **29**(3), 037302 (2012)
18. A. Kathalingam, K. Kesavan, A. Rana, J. Jeon, H.-S. Kim, Analysis of Sn concentration effect on morphological, optical, electrical and photonic properties of spray-coated Sn-doped CdO thin films. *Coatings* **8**(5), 167 (2018)
19. N.E. Makori, I.A. Amatalo, P.M. Karimi, W.K. Njoroge, Optical and electrical properties of CdO: Sn thin films for solar cell applications. *Int. J. Optoelectron. Eng* **4**(1), 11–15 (2014)
20. N.N. Jandow, H. AbuHassan, F.K. Yam, K. Ibrahim, Comparative study of the properties of ZnO thin films deposited on polypropylene carbonate (PPC) and glass substrates. *J. Mater. Sci.* **47**(4), 1972–1976 (2012)
21. L.R. de León-Gutiérrez, J.J. Cayente-Romero, J.M. Peza-Tapia, E. Barrera-Calva, J.C. Martínez-Flores, M. Ortega-López, Some physical properties of Sn-doped CdO thin films prepared by chemical bath deposition. *Mater. Lett.* **60**(29–30), 3866–3870 (2006)
22. Y.W. Zhou, X. Liu, F.Y. Wu, C.K. Zhang, X.Y. Zhang, The characteristics of $\text{CdxSn}_{1-x}\text{O}$ films prepared by RF magnetron sputtering from powder targets. *Surf. Coat. Technol.* **228**, S150–S154 (2013)
23. V. Fiorentini, A. Baldereschi, Dielectric scaling of the self-energy scissor operator in semiconductors and insulators. *Phys. Rev. B* **51**(23), 17196 (1995)
24. J. Pattar, S.N. Sawant, M. Nagaraja, N. Shashank, K.M. Balakrishna, G. Sanjeev, H.M. Mahesh, Structural optical and electrical properties of vacuum evaporated indium doped zinc telluride thin films. *Int. J. Electrochem. Sci* **4**, 369–376 (2009)
25. F.R. Chowdhury, S. Choudhury, F. Hasan, T. Begum, Optical properties of undoped and indium-doped tin oxide thin films. *J. Bangladesh Acad. Sci.* **35**(1), 99–111 (2011)
26. C.M. Ronconi, O.L. Alves, R.E. Bruns, Factorial design preparation of transparent conducting oxide thin films. *Thin Solid Films* **517**(9), 2886–2891 (2009)
27. R. Kumaravel, S. Menaka, S. Regina Mary Snega, K. Ramamurthi, K. Jeganathan, Electrical, optical and structural properties of aluminum doped cadmium oxide thin films prepared by spray pyrolysis technique. *Mater. Chem. Phys.* **122**(2–3), 444–448 (2010)

Publisher's Note Springer Nature remains neutral with regard to jurisdictional claims in published maps and institutional affiliations.